The triple GEM detector as stray neutron monitor

PUBLISHED BY IOP PUBLISHING FOR SISSA MEDIALAB

RECEIVED: *July 7, 2014*
REVISED: *October 10, 2014*
ACCEPTED: *October 13, 2014*
PUBLISHED: *November 12, 2014*

TECHNICAL REPORT

The triple GEM detector as stray neutron monitor

E. Aza,[a,b,1] **M. Magistris,**[a] **F. Murtas,**[a,c] **S. Puddu**[a,d] **and M. Silari**[a]

[a] *CERN,*
Geneva 23, 1211 Geneva, Switzerland
[b] *Department of Physics, AUTH,*
54124 Thessaloniki, Greece
[c] *LNF-INFN,*
Via Fermi 40, 00044, Frascati, Italy
[d] *AEC-LHEP, University of Bern,*
Sidlerstrasse 5, 3012 Bern, Switzerland

E-mail: eleni.aza@cern.ch

ABSTRACT: A triple GEM detector for low energy neutrons and high rejection of gamma background was tested at the CERF facility at CERN as stray neutron monitor. The detector was exposed to a wide neutron spectrum generated by a 120 GeV/c positively charged hadron beam hitting a copper target. The beam particle rate on target ranged over three orders of magnitude. The neutron count rate measured with the GEM could be linearly correlated with the beam intensity and also compared well with Monte Carlo simulations. The detector performance suggests that it can be used as an independent low energy neutron monitor at high-energy particle accelerator facilities.

KEYWORDS: Instrumentation for neutron sources; Micropattern gaseous detectors (MSGC, GEM, THGEM, RETHGEM, MHSP, MICROPIC, MICROMEGAS, InGrid, etc); Neutron detectors (cold, thermal, fast neutrons)

[1] Corresponding author.

doi:10.1088/1748-0221/9/11/T11005

Contents

1 Introduction

A triple GEM detector for low energy neutrons and high rejection of gamma background was tested at the CERF facility at CERN as stray neutron monitor. CERF (CERN-EU high-energy Reference Field) [1] is a reference radiation facility in operation since many years. The facility is served by a secondary beam from the Super Proton Synchrotron (SPS) and provides a workplace field for testing and inter-comparing various types of radiation detectors and passive dosimeters. A 120 GeV/c mixed proton/π^+ beam hits a copper target generating reference neutron spectra outside well-defined shielding configurations and a high-energy mixed stray radiation field inside the target area. The intensity of these secondary radiation fields can be varied over more than two orders of magnitude by adjusting the intensity of the beam striking the copper target. The reference beam monitor (to which all measurements performed with the various instruments are always normalized) is an air-filled, parallel-plate, transmission type ionization chamber (IC) placed in the beam a few meters upstream of the target [2]. This chamber is a very sensitive device built more than 20 years ago, specifically designed to monitor very low intensity beams. Since there is no back-up monitor, an independent monitoring of the beam intensity is usually performed by measuring the neutron dose equivalent rate at a fixed position outside the shield, using the extended-range rem counter LINUS [3, 4]. A rem counter measuring the stray neutron field, however, only provides an indication of the stability of the beam on-target (typically around 20%) and cannot be used as a reference monitor in case the IC would fail.

It has therefore been decided to investigate the use of a triple GEM [5, 6] detector designed for low energy neutrons and with high rejection of gamma background as secondary on-line monitor, measuring the low-energy neutron flux scattered from the target inside the cave. The measured neutron count rate was correlated with the IC count rate and compared with previous Monte Carlo simulations of the radiation field around the target.

2014 JINST 9 T11005

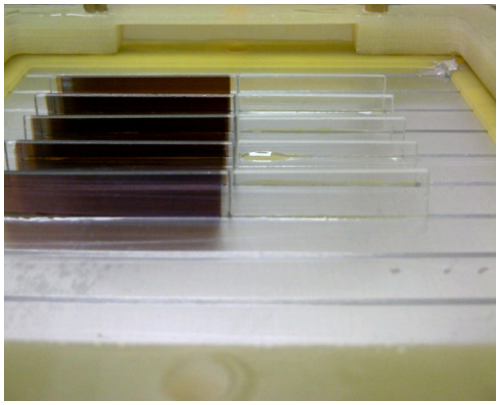

Figure 1. View of the cathode with borated glass (left) and simple glass (right).

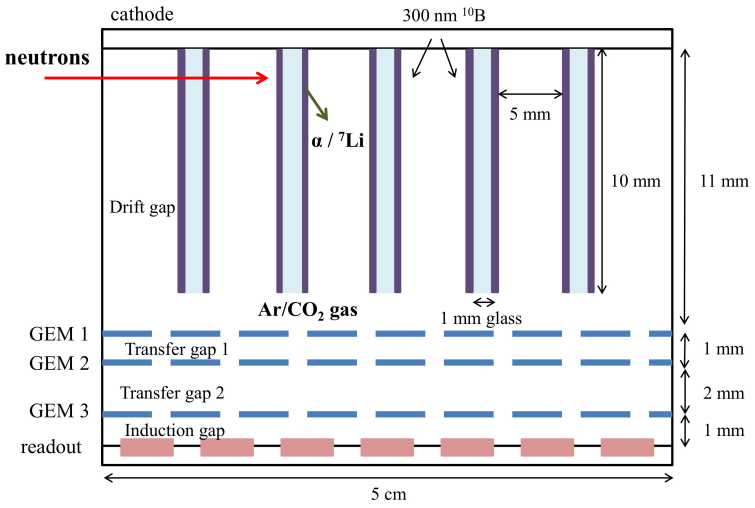

Figure 2. Layout of the Triple GEM detector. Low energy neutron conversion takes place in the borated sheets.

2 The triple GEM detector for low energy neutrons

The detector, described in detail in previous studies [7], has an active area of $5 \times 5\,\mathrm{cm}^2$ and filled with Ar/CO_2 (70/30) gas mixture (figure 1). Borated glass sheets were used for the conversion of slow neutrons; one set of five glass sheets $40 \times 10 \times 1\,\mathrm{mm}^3$ was borated with a thickness of 300 nm using an electron deposition technique and placed in the same detector with another set of five sheets, which were not borated. By having the two sets placed together it is possible to measure the difference in their performance under irradiation.

When a neutron is absorbed into the ^{10}B layer, an alpha particle, a ^{7}Li ion and usually a photon (478 keV) are produced. The charged particles highly ionize the gas mixture in the drift region of the detector thus producing secondary electrons (figure 2). These electrons drift reaching the three GEM foils where they are multiplied and finally produce a detectable signal in the induction gap. This multilayer structure offers higher conversion efficiency than a single layer, because there is higher probability of neutron interaction.

2014 JINST 9 T11005

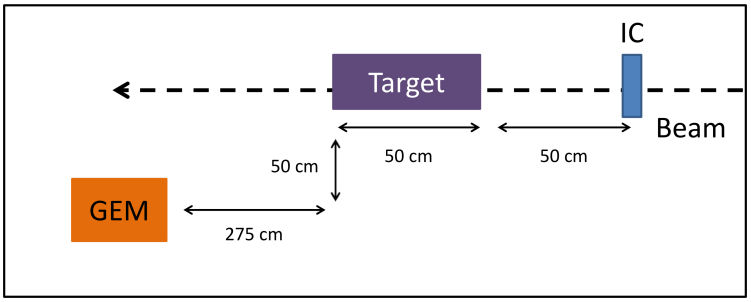

Figure 3. The experimental layout viewed from top.

The signal generated by the electron cascade is induced on a padded anode, which consists of a total of 128 pads (each of area $6 \times 3\,\mathrm{mm}^2$), organized in an 8×16 matrix. The read-out is kept at ground potential and is connected to the front-end electronics. The front-end chips used to readout the pads are the CARIOCA-GEM digital chips [8], producing LVDS time over threshold signals. All the CARIOCA chips are connected to a custom made FPGA Mother Board [9] that analyses the signal coming from them, attached to the back of the detector. The threshold set by the FPGA board to the CARIOCA chips eliminates all possible sources of electronic noise. The FPGA is able to perform counts and time measurements of discriminated signals coming from the 128 channels, allowing an external or an internal trigger. The high voltage system used to power the GEM foils is the HVGEM NIM [10], an active HV divider, whose independent channels offer higher flexibility than passive dividers. Its greatest advantage is the possibility of changing the detector gain without modifying the electric field in the gaps. The field values applied were 3, 3, 3, 5 kV/cm from drift to induction gap.

3 Experimental setup

The experimental set up at CERF is shown in figure 3, as viewed from top. The detector is placed downstream of the target at the same height, measuring the scattered radiation, whereas the IC beam monitor is just upstream of the target.

The detector was first characterized for the pad multiplicity and gain with a view to maximize the efficiency and photon rejection. The gain of the detector is an exponential function of the total voltage applied to the three foils and depends on the gas mixture. The neutron count rate measured was compared with the one from the IC and was found to have linear response with the number of beam particles on target.

3.1 Pad multiplicity

Higher multiplication and diffusion takes place with increasing voltage. The electron cluster size is also expected to increase, as it involves more neighboring pads. The cluster size was measured from the mean number of pad multiplicity by applying a time gate short enough to record only one neutron. The results are shown in figure 4 with a statistical error of 10% and indicate that the multiplicity increases rapidly with increasing voltage.

2014 JINST 9 T11005

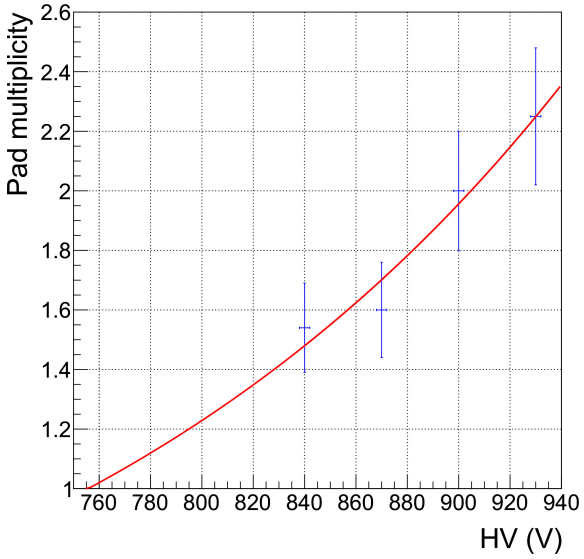

Figure 4. Pad multiplicity as a function of increasing HV.

3.2 High voltage working point

Since the detector is to be used as a neutron monitor, it is important to distinguish between neutrons and photons, i.e. between charged particles from neutron conversion and electrons from photon interactions. The photon signal is often not detected due to the threshold set to the readout chips. However, if the energy deposited by photons is high enough to generate a detectable signal, such signal cannot be distinguished from the one of alpha particles and ^{7}Li ions, because the detector cannot measure the charge.

A photon rejection technique has been introduced [11], according to which it is possible to discard the photon signal by applying suitable voltage to the foils. For this reason, two HV scans from 750 to 960 V were performed, one with a beam intensity of $5 \cdot 10^5$ s^{-1} particles on target and one with a ^{137}Cs source in order to check the difference. Neutron counts are acquired only from the borated part (figure 1), while background charged particle and photon counts are acquired on both parts. The total number of neutrons is measured by subtracting the counts from the non-borated part and dividing by the pad multiplicity.

The results from the two HV scans are shown in figure 5. Photons start being detected at 870 V, while for lower voltages the signal is derived only from neutrons. The working point was thus determined as 850 V (300-280-270 V for foils 1-2-3, respectively, see figure 2) for highest efficiency and photon rejection. According to past measurements [12], the photon sensitivity is around 10^{-7}.

The distribution of counts on the active area for low gain (820 V) is shown in figure 6a, in which the counts stem mainly from the borated sheets (right section of the detector). However, a few counts are also acquired in the non-borated sheets (left section), due to charged particles emitted by the target. For high gain (900 V, figure 6b) it is possible to see the photon contribution on the non-borated part. When the applied voltage is in the plateau region (820–870 V), the contribution from the non-borated part to the total number of counts is 15%.

2014 JINST 9 T11005

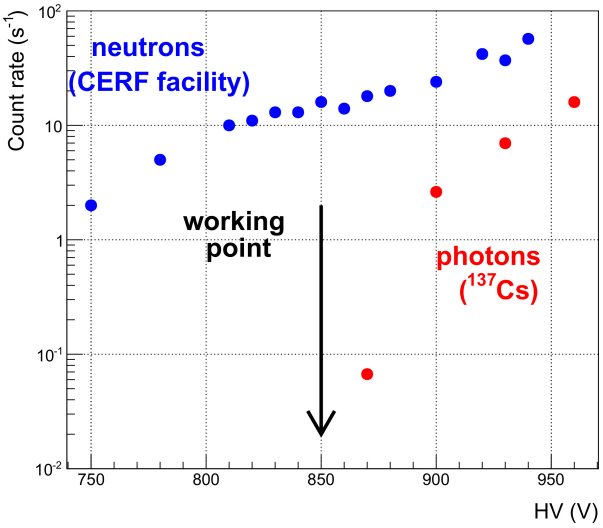

Figure 5. Number of counts measured for neutrons and photons with increasing voltage. The photon rejection is below 870 V.

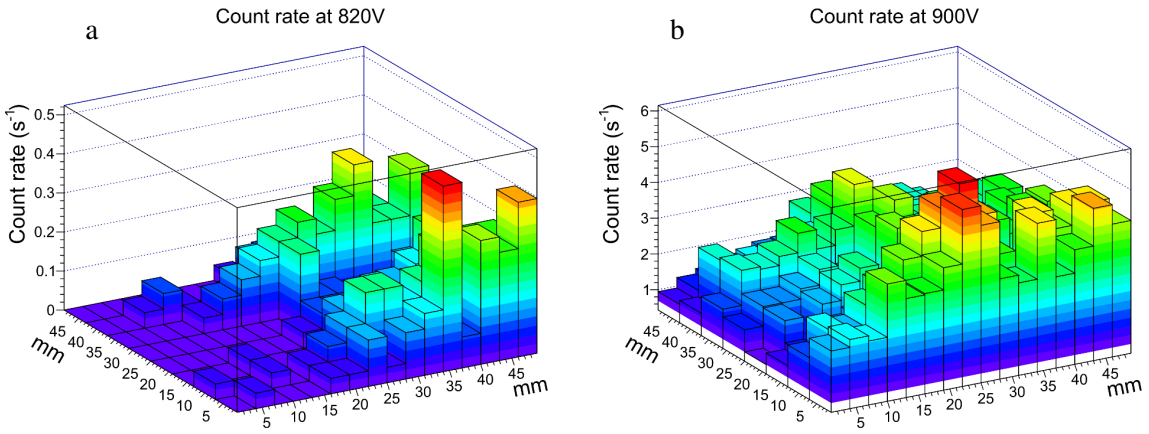

Figure 6. Count rate measured for each pad. The left section of the detector corresponds to the non-borated part and the right one to the borated one. *a*) With HV = 820 V neutrons are detected on the right section. *b*) With HV = 900 V the photon signal is detected on both sides.

3.3 Detected neutron rate

An intensity scan was performed with the flux of beam particles on the target ranging from $8 \cdot 10^4\,\mathrm{s}^{-1}$ to $2 \cdot 10^7\,\mathrm{s}^{-1}$. The time gate was set to 500 ms and the voltage applied to the foils was the working point at 850 V, corresponding to a gain of 300 [12].

The IC has a calibration factor of $(2.2 \pm 0.2) \cdot 10^4$ particles per count [2]. Good correlation was found between neutron counts and IC counts during the intensity scan resulting in the ratio 0.7 ± 0.1 neutrons per IC count, which is equivalent to $(3.3 \pm 0.1) \cdot 10^{-4}$ neutrons per particle on target per second. The results are shown in figure 7. The neutron flux measured was $(2.9 \pm 0.1) \cdot 10^3\,/\mathrm{cm}^2/\mathrm{s}$ for the highest beam intensity $(2 \cdot 10^7\,\mathrm{s}^{-1})$.

2014 JINST 9 T11005

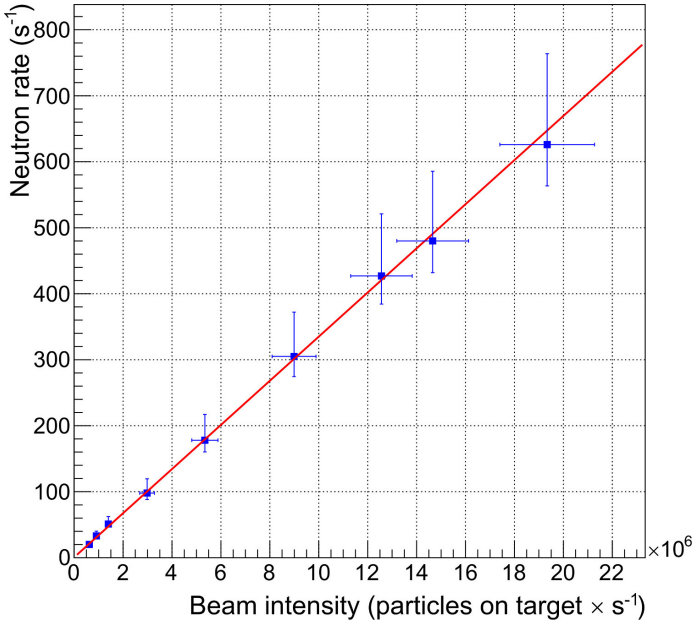

Figure 7. Neutrons rate detected per beam particle on target per second.

4 Comparison with FLUKA simulations

The experimental conditions inside the CERF target area were simulated in the past by Vincke et al. [13] with the FLUKA Monte Carlo code [14, 15] (version May 2003), in order to study the response of six air-filled ionization chambers for radiation protection applications. The six detectors were positioned around the target and the particle spectra in each of these positions were simulated. The beam energy and particle composition were the same as those of the present measurements and the estimated particle spectra were computed per primary beam particle and per unit area.

For the present measurements the GEM detector was placed in one of these positions (number 6 in ref. [13]). According to the simulations, the neutron energy in this position ranges from 0.025 eV to 20 GeV; the particle spectra are displayed in figure 8. Even though a wide variety of charged particles is present in this position, it is possible to discard their signal by subtracting the counts in the non-borated part from the counts in the borated part (figures 6a and 6b). This is a clear advantage in mixed fields such as the present case.

The mean efficiency of the detector in the neutron energy range 0.025 eV to 8.5 eV was measured as 4.3% in the TRIGA experimental facility [16]. In this energy range the TRIGA spectrum has a shape similar to the CERF spectrum (figure 9).

The total number of neutrons measured at CERF was $(2.1 \pm 0.3) \cdot 10^4$. With the detector efficiency of 4.3%, the number of impinging neutrons was estimated at $(4.9 \pm 0.8) \cdot 10^5$. The simulated number of neutrons was calculated as $(4.9 \pm 0.2) \cdot 10^5$, taking into account that the area of the device window is 2.25 cm^2. The experimental results are in very good agreement with the simulation and provide a further validation of the simulated neutron field used for instrument tests and workplace calibration.

2014 JINST 9 T11005

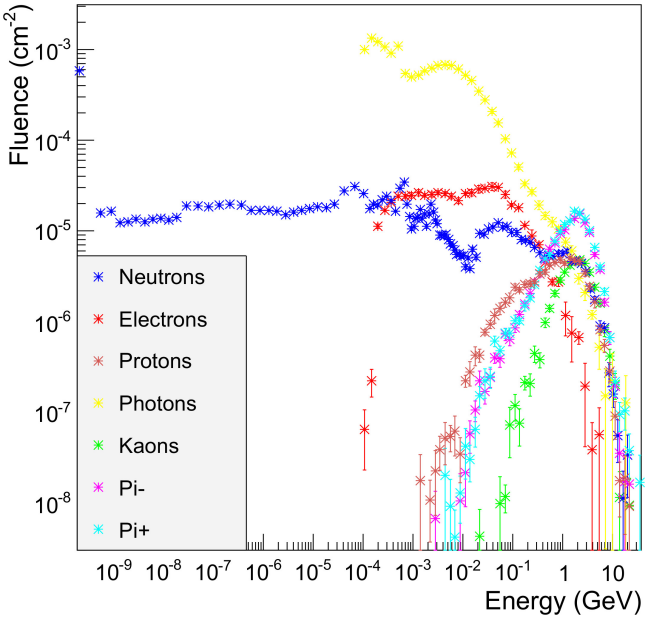

Figure 8. Particle spectra calculated with FLUKA (from [13]). Fluence is expressed in particles per cm^2 per primary beam particle. The neutron energy ranges from thermal to 20 GeV.

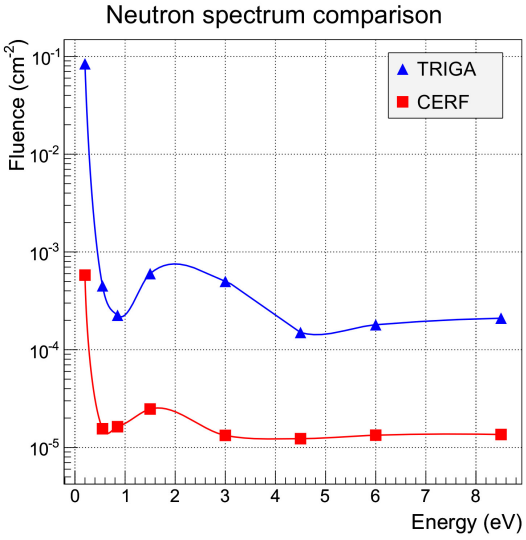

Figure 9. Neutron energy spectrum simulated at CERF [13] and determined experimentally in TRIGA [16].

5 Detector activation

Sensitivity and stability studies have shown that the detector can be activated when irradiated with a high flux of energetic particles [12]. In order to investigate this phenomenon, measurements were performed twenty-four hours after the end of the experiment. The dose rate on the GEM measured with a Geiger-Muller counter was 0.2 μSv/h, but no signal was measured with the GEM when the working HV (850 V) was applied.

2014 JINST 9 T11005

In order to detect such signal, which is probably coming from photons (gamma rays), the voltage applied to the foils was set to the maximum gain (at 1150 V). The mean counting rate from the total area was 3.2 ± 0.3 counts/s; this effect would not interfere with the neutron signal during the GEM irradiation because it can only be detected at maximum gain.

6 Conclusions

A Triple GEM detector had previously been tested as in-beam monitor of relativistic hadron beams [17]. In this work a version of the device with borated glass sheets has been successfully employed for the detection of scattered low energy neutron radiation. By applying a working HV of 850 V it is possible to reject the photon signal, while the combination of borated and non-borated glass sheets allows eliminating the signal from background charged particles, thus optimizing the ratio of signal over background.

The detector showed linear correlation with the beam intensity, with a ratio equal to $(3.3 \pm 0.1) \cdot 10^{-4}$ neutrons per beam particle impinging on the target, and corresponding to a neutron flux of $(2.9 \pm 0.1) \cdot 10^3$ /cm^2/s for the highest intensity. Considering its overall performance as a low energy neutron counter and the negligible activation, the detector can be employed as an online neutron reference counter.

Acknowledgments

The authors wish to thank Chris Theis and Helmut Vincke for providing the numerical data of figure 8.

This research project has been supported by the Marie Curie Initial Training Network Fellowship of the European Community's Seventh Framework Program under Grant Agreement PITN-GA-4 2011-289198-ARDENT.

References

[1] A. Mitaroff and M. Silari, *The CERN-EU high-energy Reference Field (CERF) facility for dosimetry at commercial flight attitudes and in space*, *Radiat. Prot. Dosimetry* **102** (2002) 7, http://rpd.oxfordjournals.org/content/102/1/7.short.

[2] A. Ferrari et al., *Monitoring reactions for the calibration of relativistic hadron beams*, *Nucl. Instrum. Meth.* **A 763** (2014) 117.

[3] C. Birattari et al., *An extended range neutron rem counter*, *Nucl. Instrum. Meth.* **A 297** (1990) 250.

[4] C. Birattari et al., *The extended range neutron rem counter 'LINUS': overview and latest developments*, *Radiat. Prot. Dosimetry* **76** (1998) 135, http://rpd.oxfordjournals.org/content/76/3/135.abstract.

[5] F. Sauli, *GEM: A new concept for electron amplification in gas detectors*, *Nucl. Instrum. Meth.* **A 386** (1997) 531.

[6] M. Alfonsi et al., *The triple-GEM detector for the M1R1 muon station at LHCb*, *IEEE Nucl. Sci. Symp. Conf. Rec.* **2** (2005) 811.

2014 JINST 9 T11005

[7] A. Pietropaolo et al., *A new ^{3}He-free thermal neutrons detector concept based on the GEM technology*, *Nucl. Instrum. Meth.* **A 729** (2013) 117.

[8] W. Bonivento et al., *Development of the CARIOCA front-end chip for the LHCb muon detector*, *Nucl. Instrum. Meth.* **A 491** (2002) 233.

[9] F. Murtas et al., *Applications in beam diagnostics with triple GEM detectors*, *Nucl. Instrum. Meth.* **A 617** (2010) 237.

[10] G. Corradi, F. Murtas and D. Tagnani, *A novel high-voltage system for a triple GEM detector*, *Nucl. Instrum. Meth.* **A 572** (2007) 96.

[11] B. Esposito et al., *Design of a GEM-based detector for the measurement of fast neutrons*, *Nucl. Instrum. Meth.* **A 617** (2010) 155.

[12] G. Croci et al., *Measurements of γ-ray sensitivity of a GEM based detector using a coincidence technique*, 2013 *JINST* **8** P04006.

[13] H. Vincke et al., *Simulation and measurements of the response of an air ionization chamber exposed to a mixed high-energy radiation field*, *Radiat. Prot. Dosimetry* **116** (2005) 380.

[14] A. Ferrari et al., *FLUKA: a multi-particle transport code*, CERN-2005-010 [INFN-TC-2005-11] [SLAC-R-773] (2005).

[15] G. Battistoni et al., *The FLUKA code: Description and benchmarking*, *AIP Conf. Proc.* **896** (2007) 31.

[16] F. Murtas, *Applications of triple GEM detectors beyond particle and nuclear physics*, 2014 *JINST* **9** C01058.

[17] E. Aza et al., *The triple GEM detector as beam monitor for relativistic hadron beams*, 2014 *JINST* **9** P06006.

2014 JINST 9 T11005